Supporting Information

Pascal et al. 10.1073/pnas.1300619110

SI Text

SI Methods

Mathematical Modeling of Tumor Kill. We study passive drug diffusion across tumor tissue after extravasation from a cylindrical source, for example, a blood vessel segment, described by a diffusion-reaction mass conservation equation in cylindrical coordinates (Fig. 2), assuming that the length of the blood vessel segment, h, is much greater than the diffusion penetration length, L (1):

$$\frac{1}{r}\frac{\partial}{\partial r}\left(r\frac{\partial \sigma}{\partial r}\right)-\frac{\sigma}{L^2}=0, \qquad \text{[S1]}$$

where r is the radial coordinate scaled with the diffusion penetration length $L=\sqrt{D/\lambda}$, D is the diffusivity of the drug (a constant assuming for simplicity that the tumor microenvironment is isotropic), σ is the local concentration of drug, and λ the cellular uptake rate of drug (inverse time). Bessel's differential Eq. **S1** has solution (2):

$$\sigma=c_1\cdot I_0(r/L)+c_2\cdot K_0(r/L), \qquad \text{[S2]}$$

where I_0 and K_0 are modified Bessel functions of the first and second kinds of order zero. Because I_0 increases monotonically, it does not represent a valid solution, under the additional assumption $L \ll H$, where H is the size of the computational domain, for example, the interportal distance in the liver (Fig. 2). Applying the boundary condition at the source's radius r_b that the intravascular drug concentration is σ_0,

$$\sigma(r=r_b)=\sigma_0, \qquad \text{[S3]}$$

a solution for the concentration distribution of drug within the tumor can be obtained:

$$\frac{\sigma}{\sigma_0}=\frac{K_0(r/L)}{K_0(r_b/L)}. \qquad \text{[S4]}$$

The fraction of tumor killed can then be determined by the following volume average (3) over the region of dead tumor surrounding the blood source (Fig. 2*B*, red dashed line):

$$f_{\text{kill}}=\frac{2\cdot\pi\cdot h}{V_{\text{tot}}}\cdot\int_{r_b}^{r_k} f_{\text{kill}}^{\text{M}}(\sigma(r))\cdot r\cdot \mathrm{d}r, \qquad \text{[S5]}$$

where r_k is the thickness of the region of dead tumor, h is the length of the blood source, $f_{\text{kill}}^{\text{M}}(\sigma)$ is the fraction of tumor cells killed in a monolayer cytotoxicity experiment, which is dependent on the local concentration of drug, σ, and V_{tot} is the total volume of tumor served by the blood source. Assuming that the blood sources are uniformly distributed throughout the tumor, the total volume served by a source is

$$V_{\text{tot}}=\frac{V_{\text{tumor}}}{N_{\text{vessels}}}=\frac{V_{\text{tumor}}}{V_{\text{vessels}}}\cdot\frac{V_{\text{vessels}}}{N_{\text{vessels}}}, \qquad \text{[S6]}$$

where $\frac{V_{\text{vessels}}}{V_{\text{tumor}}}$ is the blood volume fraction BVF and $\frac{V_{\text{vessels}}}{N_{\text{vessels}}}$ is the volume of a single cylindrical blood source of radius r_b. Thus, the total volume of tumor served by the source as a function of blood volume fraction and portal radius is

$$V_{\text{tot}}=\frac{\pi\cdot r_b^2\cdot h}{\text{BVF}}. \qquad \text{[S7]}$$

Substituting Eq. **S7** into Eq. **S5** gives

$$f_{\text{kill}}=\frac{2\cdot\text{BVF}}{r_b^2}\cdot\int_{r_b}^{r_k} f_{\text{kill}}^{\text{M}}(\sigma(r))\cdot r\cdot \mathrm{d}r \qquad \text{[S8]}$$

for the predicted fraction of tumor volume killed.

Here, we approximate the fraction of tumor cells killed in a monolayer cytotoxicity assay, that is, in the absence of diffusion gradients, $f_{\text{kill}}^{\text{M}}(\sigma)$, with a piecewise linear function (4):

$$f_{\text{kill}}(\sigma)=f_{\text{kill}}^{\text{M}}(\sigma_0)\cdot\frac{\sigma(r)-\sigma_k}{\sigma_0-\sigma_k}, \qquad \text{[S9]}$$

($f_{\text{kill}}(\sigma)=0$ for $\sigma(r)<\sigma_k$), where $\sigma_k=\sigma(r_k)$ is the threshold drug concentration at which the tumor cells are killed in response to the drug, given as $\frac{\sigma_k}{\sigma_0}=\frac{K_0(r_k/L)}{K_0(r_b/L)}$ (Eq. **1b**) and $f_{\text{kill}}^{\text{M}}(\sigma_0)$ is the fraction of cells killed by a clinically relevant dosage of drug in a monolayer experiment. K_0 and K_1 are modified Bessel functions of the second kind of orders 0 and 1, respectively (2). Substituting Eq. **S9** and the expression for the threshold drug concentration, σ_k, into Eq. **S8** gives

$$f_{\text{kill}}=\frac{2\cdot\text{BVF}\cdot f_{\text{kill}}^{\text{M}}(\sigma_0)}{r_b^2}\cdot\int_{r_b}^{r_k}\frac{K_0(r/L)-K_0(r_k/L)}{K_0(r_b/L)-K_0(r_k/L)}\cdot r\cdot \mathrm{d}r. \qquad \text{[S10]}$$

Performing the integration leads to the fraction of tumor volume killed, f_{kill}, of Eq. **1a**, as a function of BVF, thickness of dead tumor region r_k, drug source radius r_b, and fraction of cells killed in a monolayer cytotoxicity experiment $f_{\text{kill}}^{\text{M}}(\sigma_0)$, all of which can be directly measured to inform the model.

Note that Eq. **1a** does not have the correct limit as the diffusion penetration length L approaches infinity. Without uptake of drug, the physically correct steady-state solution for drug concentration (i.e., independent of time) should be a constant $\sigma=\sigma_0$ throughout the tumor tissue, whereas our solution decays at large distances from the source. Our solution Eq. **1a** is a good approximation when L is small compared with the interportal distance H. This assumption is valid as we found in a regression analysis L = 191 μm (main text), whereas H = 0.5 mm.

Histopathology Measurements. The accuracy of the image segmentation procedure is demonstrated in Fig. S1 by comparing the distribution of f_{kill} values from histopathology of the third cohort of patients [MD Anderson Cancer Center (MDACC)], measured using the GNU Image Manipulation Program (GIMP) by the University of New Mexico group, with those directly assessed by the pathologist at MDACC.

Regression and Statistical Analyses. Least-squares fitting of Eq. **1a** was performed to the kill fraction and kill radii measured in liver metastasis in the Cooperative Human Tissue Network (CHTN) patient cohort (first cohort; Fig. 4). The goal of the statistical analysis was to assess the equivalence (5), between the patient tissue histopathology data of kill ratio f_{kill} in colorectal cancer (CRC) metastatic to liver from CHTN (experimental group), and the outputs of the mathematical model from Eq. **1a** (computational

group) as shown in Fig. 4. We first performed a student t test, with the null hypothesis that the means of the two groups, patient data vs. model, were statistically the same (6, 7). This t test demonstrated no statistically significant difference between the two groups. We then performed the equivalence test (8–10) based on defining an equivalence margin (i.e., the range of values for which data groups are "close enough" to be considered equivalent) (11). We also determined that our sample size was sufficient to have confidence in these results.

i) Independent two-sided two-sample student's t-test: We used a standard significance level $\alpha = 0.05$ (6, 7) and obtained a P value of 0.46, confirming that the difference between the two groups was statistically not significant (i.e., the t test results were not sufficient to reject the null hypothesis) (6, 7).

ii) Equivalence test: We used a standard two-sided significance level $\alpha = 0.05$, power $\beta = 0.8$, and equivalence margin = 20% (the SD of the experimental group data were $\sigma_d = 0.189$) of the mean of measured f_{kill} values, that is, $0.363 \times 20\% = 0.073$, generating a range of [–0.073, 0.073]. We set the equivalence margin as 20% following standard procedures in clinical research (12, 13). Once the equivalence margin was set, we used the two-sided confidence interval approach (5, 14–16) to test for equivalence. Following the procedure described elsewhere (5, 14–16) for calculating the confidence interval based on the SE for the difference between the means of f_{kill} for the computational and experimental groups, we found the 95% confidence interval of [-0.027, 0.059], which lies within the range of the equivalence margin above, thus verifying that the two groups can be considered equivalent with 95% confidence, once proven that the sample size is adequate.

iii) Test of sample size: Each group had a sample size of 147 (a total of 49 images from the eight patients with three measurements per image used for the analysis, $49 \times 3 = 147$). Each square image from the histopathology had a side length $>L$ to ensure that the diffusion fields of the images would be uncorrelated. Following standard procedure (17), we confirmed that the sample size used in the equivalence test described above was sufficient to claim equivalence between the two groups. We calculated the required sample size as (17) $N_d = \frac{2\sigma_d^2(Z_\alpha + Z_\beta)^2}{\delta_d^2}$, where N_d is the sample size, σ_d the SD of the experimental group data, δ_d the equivalence margin, and Z_α and Z_β are constants corresponding to the desired level of significance $\alpha = 0.05$ and desired power $\beta = 0.8$. In our analysis, $\sigma_d = 0.189$, $\delta_d = 0.073$, $Z_\alpha = 1.96$, and $Z_\beta = 0.84$. The resulting required sample size was $N_d = 105$ for each group, less than the actual sample size of 147, demonstrating equivalence between the two groups at the 0.05 significance level.

Test of Model Predictivity. To obtain Eq. **3** for the maximum f_{kill}, we perform the integration **[S10]** for $r_k = r_b/\sqrt{\text{BVF}}$, that is, assuming that the drug action extends throughout the entire volume **[S7]** served by each drug source. This assumption is corroborated in Fig. S2, where Eq. **3** is fit to the average measurement of tumor kill in each of the four glioblastoma multiforme (GBM) patients (second cohort). The parameter $\langle r_b/L \rangle$ thus calculated is in agreement with the direct measurement (Fig. S2, *Inset*).

Prospective Application of the Model Based on Pretreatment Computed Tomography Scans. The linear regression analysis illustrating significant correlation of the measurements of BVF performed from posttreatment histology to the computed tomography (CT) measurements (Hounsfield units) at the arterial phase performed before treatment for the third cohort of patients (MDACC) is shown in Fig. S3 and leads to Eq. **4**.

SI Results

Fitting the Mathematical Model to Patient Data by a Regression Analysis Identifies Biologically Realistic Parameter Values. Fig. S4 validates the scaling for the BVF parameter estimated by calculating the ratio between the portal and lobule volumes in the liver: $\text{BVF} \propto 4\pi/(3\cdot\sqrt{3})\cdot(r_b/H)^2$ (main text).

Validation of the Model in a Different Tumor Type. Fig. S5 shows the comparison of predictions of patient-specific cell kill from Eq. **1a** to the direct measurements from histopathology of GBM in three additional patients of a cohort biopsied after chemotherapy (Fig. 5).

1. Bird RB, Stewart WE, Lightfoot EN (2007) *Transport Phenomena* (Wiley, New York).
2. Kreyszig E (2010) *Advanced Engineering Mathematics* (Wiley, New York).
3. Stewart J (2008) *Calculus* (Brooks/Cole, Pacific Grove, CA).
4. Frieboes HB, et al. (2009) Prediction of drug response in breast cancer using integrative experimental/computational modeling. *Cancer Res* 69(10):4484–4492.
5. GraphPad Software (2007) GraphPad Prism, Version 5.0, Statistics Guide. Available at www.graphpad.com/downloads/docs/Prism5Stats.pdf.
6. Altman DG, Bland JM (1995) Absence of evidence is not evidence of absence. *BMJ* 311(7003):485.
7. Costa LJ, Xavier AC, del Giglio A (2004) Negative results in cancer clinical trials—equivalence or poor accrual? *Control Clin Trials* 25(5):525–533.
8. Hoenig JM, Heisey DM (2001) The abuse of power: The pervasive fallacy of power calculations for data analysis. *Am Stat* 55(1):19–24.
9. Greene WL, Concato J, Feinstein AR (2000) Claims of equivalence in medical research: Are they supported by the evidence? *Ann Intern Med* 132(9):715–722.
10. Moher D, Dulberg CS, Wells GA (1994) Statistical power, sample size, and their reporting in randomized controlled trials. *JAMA* 272(2):122–124.
11. Walker E, Nowacki AS (2011) Understanding equivalence and noninferiority testing. *J Gen Intern Med* 26(2):192–196.
12. Piaggio G, Elbourne DR, Altman DG, Pocock SJ, Evans SJ; CONSORT Group (2006) Reporting of noninferiority and equivalence randomized trials: an extension of the CONSORT statement. *JAMA* 295(10):1152–1160.
13. Ware JH, Antman EM (1997) Equivalence trials. *N Engl J Med* 337(16):1159–1161.
14. Fleming TR (2000) Design and interpretation of equivalence trials. *Am Heart J* 139(4): S171–S176.
15. Jones B, Jarvis P, Lewis JA, Ebbutt AF (1996) Trials to assess equivalence: the importance of rigorous methods. *BMJ* 313(7048):36–39.
16. Rothman KJ (1986) Significance questing. *Ann Intern Med* 105(3):445–447.
17. Friedman LM, Furberg CD, DeMets DL (2010) *Fundamentals of Clinical Trials* (Springer, New York), 4th Ed.

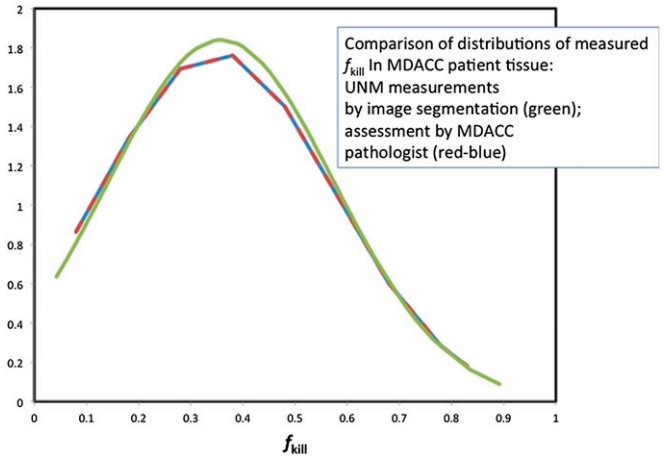

Fig. S1. Comparison of distributions of measured f_{kill} in tissue from the third cohort of 15 MDACC patients. Measurements by image segmentation using the GIMP software (1) (green); standard clinical assessment by the pathologist at MDACC (red and blue).

1. The GIMP Team (2013) GNU Image Manipulation Program. Available at http://docs.gimp.org/odftest/en.pdf.

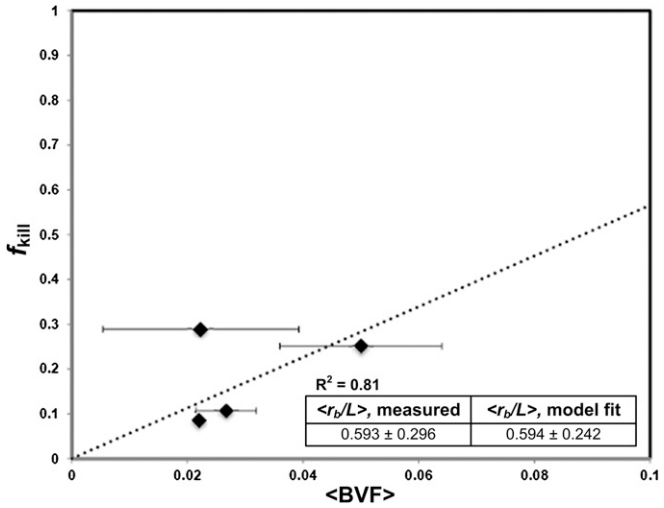

Fig. S2. Regression analysis of Eq. **3** (dotted line). Direct measurements of fraction of tumor kill f_{kill} and average blood volume fraction BVF from GBM histopathology of four patient biopsies after chemotherapy (symbols with SD). Comparison of dimensionless blood vessel radius parameter $< r_b/L >$ calculated from the fit and directly measured from the histopathology (*Inset*).

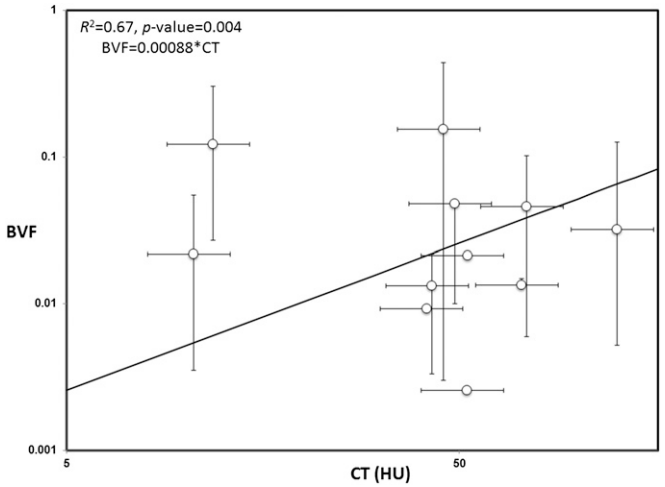

Fig. S3. BVF (with SD) measured from histopathology vs. arterial-phase contrast-enhanced CT data (with SD) from patients with CRC metastatic to liver (log-scale axes). The fit provides Eq. **4**. SD for the CT data were estimated from the measurements of contrast enhancement of the aorta and represents 25% variability in physiology and contrast-injection protocols across patients.

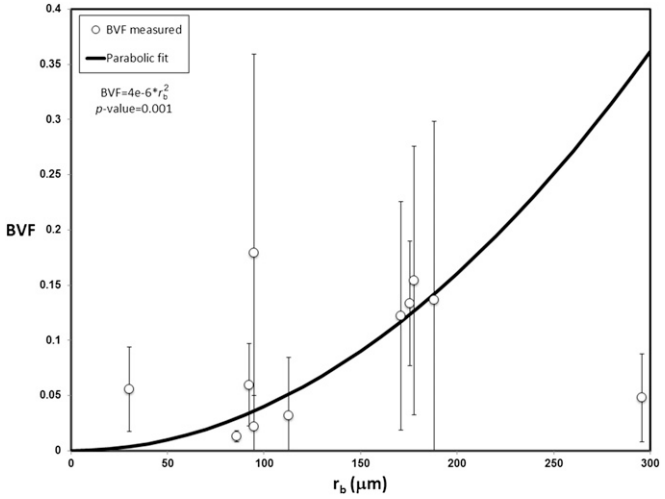

Fig. S4. BVF vs. r_b measured from histopathology of third cohort of patients with CRC metastatic to liver (MDACC). The fit validates the scaling $BVF \propto 4\pi/(3\cdot\sqrt{3})\cdot(r_b/H)^2$ (main text).

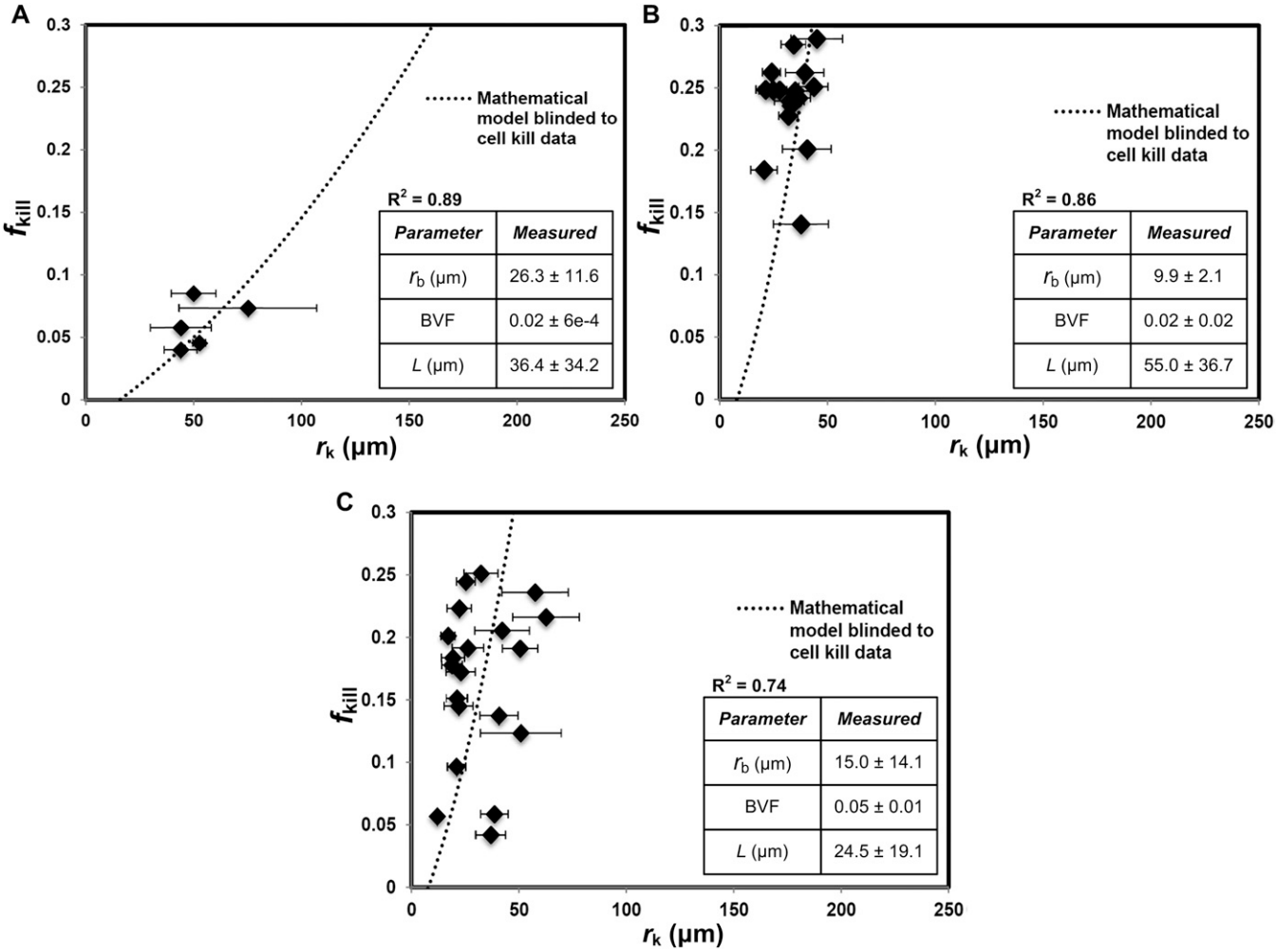

Fig. S5. Three additional cases for validating the model in GBM. Patient-specific predictions of Eq. **1a** (dotted line) vs. direct measurement of fraction of tumor kill f_{kill} (and kill radius r_k) from histopathology of patient biopsies after chemotherapy (symbols with error bars for SDs). Patient (*A*): six images, 66 measurements total; (*B*) 18 images, 200 measurements total; and (*C*): 22 images, 312 measurements total. (*Insets*) Input parameters BVF and r_b measured from histopathology. Parameter *L* (drug diffusion penetration distance) was calculated using Eq. **3** from the measurements of the other parameters (*Methods*).